Case report

Pediatric chordoma associated with tuberous sclerosis complex: A rare case report with a thorough analysis of potential therapeutic molecular targets

Kirill Anoshkin [a,*], Denis Zosen [b], Kristina Karandasheva [a], Maxim Untesco [c,d], Ilya Volodin [a], Ekaterina Alekseeva [a,e], Anna Parfenenkova [f], Eugenia Snegova [g], Aleksandr Kim [h], Marina Dorofeeva [i], Sergei Kutsev [a], Vladimir Strelnikov [a]

[a] Research Centre for Medical Genetics, Moskvorechye Str. 1, 115522 Moscow, Russia
[b] Faculty of Mathematics and Natural Sciences, University of Oslo, PO Box 1068, Blindern, 0316 Oslo, Norway
[c] UNIM LLC, Podsosensky Lane 23, 105062 Moscow, Russia
[d] Pathology Department, Telemark HF Hospital, Ulefossveien 55, PO Box 2900 Kjørbekk, 3710 Skien, Norway
[e] I.M. Sechenov First Moscow State Medical University (Sechenov University), Trubetskaya Str. 8-2, 119991 Moscow, Russia
[f] Saint Petersburg State University, University emb. 7-9, 199034 Saint Petersburg, Russia
[g] Saint Petersburg State Budget Healthcare Facility "Advisory and Diagnostic Center for Children", Oleko Dundicha Str. 36/2, 192289 Saint Petersburg, Russia
[h] Almazov National Medical Research Centre, Akkuratova Str. 2, 197341 Saint Petersburg, Russia
[i] Veltischev Research and Clinical Institute for Pediatrics of the Pirogov Russian National Research Medical University, Taldomskaya Str. 2, 125412 Moscow, Russia

ARTICLE INFO

ABSTRACT

Chordoma associated with tuberous sclerosis complex (TSC) is an extremely rare tumor that was described only in 13 cases since 1975. Chordoma itself is a malignant slow-growing bone tumor thought to arise from vestigial or ectopic notochordal tissue. Chordoma associated with TSC differs from chordoma in the general pediatric population in the median age, where the diagnosis of TSC-associated chordoma is 6.2 months, whereas for chordoma in the general pediatric population it is set to 12 years. The majority of TSC-associated chordomas are localized in skull-based and sacrum regions, and rare in the spine. Chordomas are genetically heterogeneous tumors characterized by chromosomal instability (CIN), and alterations involving PI3K-AKT signaling pathway genes and chromatin remodeling genes. Here we present the 14th case of chordoma associated with TSC in a 1-year-old pediatric patient. Alongside biallelic inactivation of the *TSC1* gene, molecular genetic analysis revealed CIN and involvement of epigenetic regulation genes. In addition, we found the engagement of *CBX7* and apolipoprotein B editing complex (APOBEC3) genes that were not yet seen in chordomas before. Amplification of *CBX7* may epigenetically silence the *CDKN2A* gene, whereas amplification of *APOBEC3* genes can explain the frequent occurrence of CIN in chordomas. We also found that *KRAS* gene is located in the region with gain status, which may suggest the ineffectiveness of potential EGFR monotherapy. Thus, molecular genetic analysis carried out in this study broadens the horizons of possible approaches for targeted therapies with potential applications for personalized medicine.

1. Introduction

Chordomas are malignant slow-growing bone tumors thought to arise from vestigial or ectopic notochordal tissue [1]. The incidence of sporadic chordomas is very rare and is currently estimated to be 0.8 cases per 1 million/year, which is lower than Ewing's sarcoma (1.7–4.4 cases per 1 million/year) [1, 2]. In the majority of cases, chordomas occur in people 40–60 years of age and have a slight predominance in males [1]. Extremely rare chordomas are observed in such diseases as

tuberous sclerosis complex (TSC). Since 1975, 13 cases have been described so far [3].

Recent studies show that chordomas associated with TSC have a silent tumor burden and eventually harbor mutations in TSC genes (in the latest article – biallelic inactivation of *TSC1* gene) [3]. However, due to its rarity, the number of studies dedicated to molecular genetic analyses of these tumors associated with TSC is very limited. On the contrary, molecular genetic analysis of sporadic chordomas shows that these tumors mostly harbor chromosomal instability (CIN), alterations that involve

---

* Corresponding author.
E-mail address: anoshkinki@gmail.com (K. Anoshkin).

PI3K-AKT signaling pathway genes and chromatin remodeling genes [4]. Also, a recent study shows that altered genes *PBRM1*, *SETD2*, *CDKN2A/B*, and *LYST* account for approximately 34% of the analyzed chordoma cohort [4].

Due to its genetic heterogeneity, numerous clinical trials of targeted therapies are currently underway and new approaches for treating chordomas are being suggested [5, 6, 7]. Nevertheless, the most effective treatment for chordomas is wide excision with adequate margins [8, 9]. Molecular genetic characterization by means of high-throughput sequencing (HTS) and chromosomal microarray analysis (CMA) will add to a better understanding of TSC-associated pediatric chordoma pathology, its molecular signatures and potential therapeutic targets. Here we present the 14th case of clivus chordoma in the pediatric patient with autosomal dominant disease TSC with a microscopic and immunohistochemical examination, new molecular genetic findings by profiling 409 tumor-related genes and CMA.

1.1. Case presentation

A 12-month-old Caucasian boy was admitted to the Consultative and Diagnostic Center for Children, Saint Petersburg, Russia in 2020, with complaints of convulsive seizures in the form of faltering, smirking with the withdrawal of the head and eyes, lasting 3–4 s. At 28 weeks' gestation, an ultrasound revealed cardiac rhabdomyoma and a fetal MRI scan suspected a possible TSC pathology (Figure 1A–F). The baby was born in time, 3250 g, 51 cm, and 7/9 Apgar score. No evidence or cases of TSC/chordoma were seen in the family history.

At birth, the boy had a blond hair strand, polydactyly of the right hand, and rhabdomyoma of the heart. At four months of age, depigmented spots appeared on the torso and the diagnosis of TSC was clinically confirmed. The child's psychomotor development was according to age, with no focal neurological symptoms on examinations. Convulsive seizures were first noted at the age of 8 months and then recurred two months later, antiepileptic therapy has been initiated. A brain CT scan showed a massive neoplasm formation in the posterior cranial fossa, tubers, triventricular hydrocephalus and arachnoid cyst of the left temporal region. A brain MRI with contrast (Figure 1E and F) confirmed an extracranial solid mass in the posterior fossa with brain stem compression; subcortically, in the white matter of the frontal lobes, and periventricularly – defined tubers (Figure 1B and C); triventricular hydrocephalus and arachnoid cyst of the left temporal region. Diagnosis by a neurologist: TSC with symptomatic epilepsy, - the child was referred to a neurosurgeon. The pathogenic mutation in the *TSC1* gene 15 exon c.1690 G > T, p.E564* has been detected with molecular genetic analysis of the blood sample.

At 13 months of age, microsurgical resection of an extracranial tumor and subsequent histological examination confirmed clivus chordoma at the Almazov National Medical Research Centre, St. Petersburg, Russia, no metastases were observed. A follow-up brain MRI scan at the age of 1.5 years revealed a continued growth of the tumor – increased thickness of an extracranial mass on the left side. Pathological tissue of heterogeneous structure, not accumulating contrast, 4.6 × 2.2 × 4.4 mm (previously: 4.6 × 1.8 × 4.4 mm) was visualized starting from the clivus of the sphenoid bone and extending to the apex of the odontoid process.
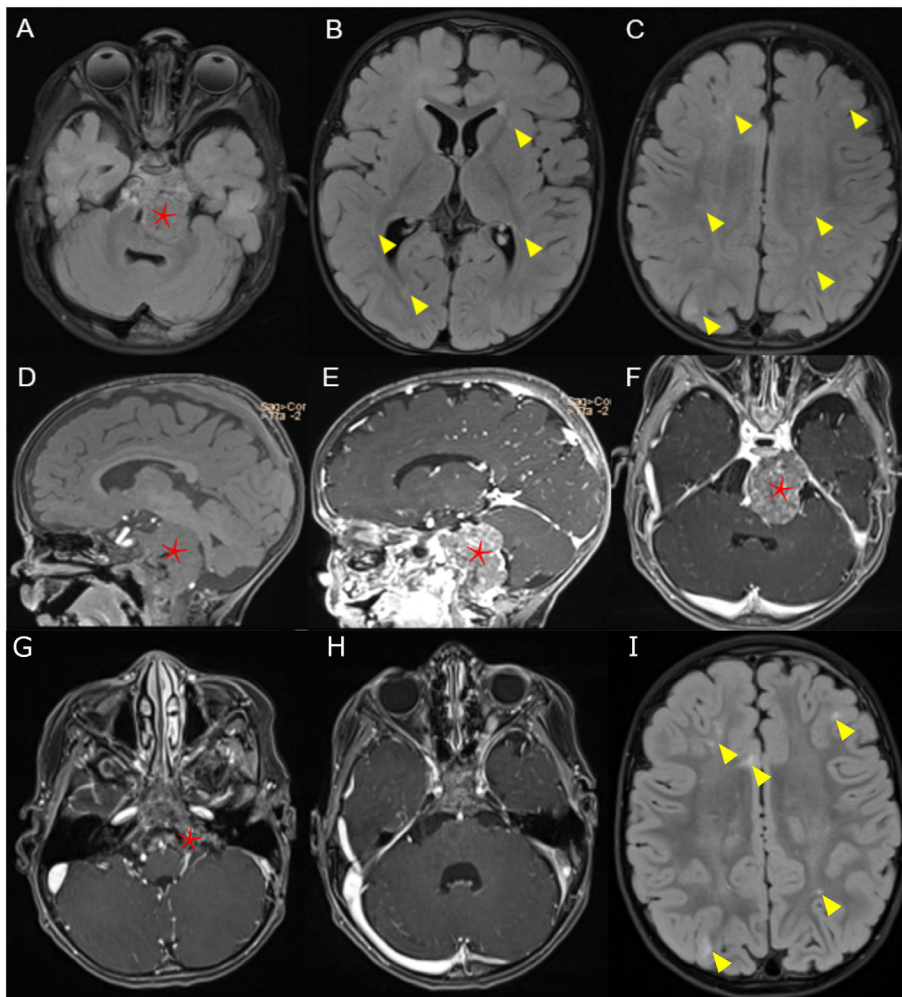
Figure 1. Patient's preoperative (A–F) and postoperative (G–I) structural MRI examination. Clivus chordoma is marked with red asterisks, hyperintense signals are marked with yellow arrows. (A–C) T2-weighted MRI scan in the axial projections. (A) clivus chordoma. (B-C, I) MRI FLAIR sequence showing the focus of hyperintense signals in the white matter, features being consistent with the diagnosis of tuberous sclerosis. (D–F) T2-weighted MRI of a clivus chordoma. (D) sagittal plane with no contrast. (E) sagittal and (F) axial planes with contrast. (G, H) T1-weighted MRI scan in the axial projections. (I) MRI FLAIR sequence.

1.2. Treatment and follow-up

Symptomatic antiepileptic drug treatment and proton radiation therapy were performed and two months later, at 2 years of age, a postoperative brain MRI scan showed a reduction in the size of the tumor (Figure 1G and H), while tubers stayed present (Figure 1I). At this moment, the patient has no clinical manifestations of the disease. Based on the obtained diagnostic data, it's planned to continue monitoring the patient, and adjust antiepileptic therapy if necessary.

2. Materials and methods

2.1. Ethical statement

The study was conducted according to the guidelines of the Declaration of Helsinki, and approved by the Ethics Committee at the Research Centre for Medical Genetics, Moscow, Russia. The patient's guardian signed the informed consent to undergo diagnostic procedures and treatment, as well as to participate in the study, and presentation of clinical and molecular data in the scientific and medical literature.

2.2. Sample preparation and histopathology

Surgical specimen consisting of tumor fragments was entirely fixed in 10% buffered formalin. Formalin-fixed paraffin-embedded (FFPE) tissue blocks were prepared after a standard processing procedure. Hematoxylin and Eosin (H&E) slides were prepared for diagnostic purposes. Additional tissue sections were made for immunohistochemistry and molecular genetic studies. Immunohistochemical stains were performed on BOND-MAX automated staining system, using standardized protocols with BOND Epitope Retrieval solutions 1/2 and BOND Polymer Refine Detection Kit, all from Leica Biosystems, Germany. Antibodies used, are as follows: Pan-Cytokeratin (Leica Biosystems, cat.№ PA0094), CD68 (Leica Biosystems, cat.№ NCL-L-CD68), Brachyury (Abcam, cat.№ ab209665), EMA (Biogenex, cat.№ AMB78-5M), S100 (CellMarque, cat.№ 330M-16), GFAP (Leica Biosystems, cat.№ NCL-L-GFAP-GA5), Ki67 (Leica Biosystems, cat.№ PA0118). Immunohistochemical stains were performed using standard staining protocols and according to antibody vendor recommendations. All histological slides were scanned at 200× absolute magnification using the Aperio AT2 scanning system (Aperio Technologies, Vista, CA). Acquired digital pathology slides images were uploaded and analyzed on the Digital Pathology viewing platform by two specialists. Morphology was assessed directly on the screen. Mitotic count was performed on a virtual circular area with a diameter of 500 μm (average diameter of a microscopic field at ×400 magnification). Proliferation index Ki67 immunostaining morphometric analysis was performed using an integrated proprietary Ki67 assessment algorithm (UNIM LTD, Moscow, Russia): an area was considered acceptable for analysis if it contained 500–1000 tumor cells. The Ki67 index is the ratio of the number of tumor cells with positive nuclear Ki67 staining to the total number of tumor cells in a designated area. Three areas with the highest positive nuclear staining cell ratio were designated as hotspot areas. These areas were then analyzed, and a mean value of measurements was calculated.

2.3. High-throughput sequencing (HTS) and therapeutic biomarkers assessment

DNA was extracted from FFPE tumor tissue using GeneRead DNA FFPE kit (Qiagen, cat.№ 180134). DNA sequencing (HTS) was performed by using Ion AmpliSeq targeted amplification technology with Ion AmpliSeq Comprehensive Cancer Panel (Thermo Fisher Scientific, cat.№ 4477685), Oncomine Tumor Mutation Load Assay (Thermo Fisher Scientific, cat.№ A37909) and a custom panel including 25 genes involved in epigenetic regulation (Supplementary Material) on Ion S5™ System (Thermo Fisher Scientific, USA). All found point mutations were verified by Sanger sequencing (Supplementary Material). PCR parameters for

TERT promoter mutations C250T and C228T and MGMT methylation status are described in Supplementary Material.

2.4. Chromosomal microarray analysis (CMA)

For the detection of chromosomal aberrations, we used SNP-array OncoScan (Thermo Fisher Scientific, cat. № 902695) on GeneChip Scanner 3000 7G System (Applied Biosystems, cat.№ 00–0213), following the manufacturer's recommendations. The data were analyzed with Chromosome Analysis Suite (ChAS) 4.2 software (Affymetrix) and OncoScan default settings. All copy number alterations were manually reviewed.

2.5. Bioinformatic analysis

The bioinformatics workflow for sequencing data analysis was based on Torrent Suite software (version 5.10.1). Annotation was performed by ANNOVAR [10]. Filtration of pathogenic mutations was made with the following parameters: read depth ≥250×, variant allele fraction (VAF) > 5%, strand bias is excluded, occurrence in the population <1% (gnomAD). All filtered point mutations were manually reviewed using Integrative Genomics Viewer (IGV) [11]. Tumor mutation burden (TMB) was determined using the Oncomine Tumor Mutation Load Assay panel (Thermo Fisher Scientific, cat.№ A37909) in Ion Reporter software. For pathway enrichment analysis, we used data from CMA, excluded oncogenes that were in loss regions and tumor suppressor genes that were in gains regions, and performed analysis using the ClusterProfiler R package version 3.18.1 [12].

3. Results

3.1. Histology and immunohistochemistry

Histologically, conventional chordoma morphology was observed: tumor presented a solid lobulated growth pattern, with cords and nests of large epithelioid cells with clear or slightly eosinophilic, bubbly cytoplasm ("physaliphorous" cells). Cells were focally embedded in a moderate amount of chondromyxoid stroma (Figure 2A and B). Tumor lobules were divided by fibrous septa rich in prominent blood vessels and dense lymphoplasmacytic inflammatory infiltrate. Cytologic atypia varied from moderate to severe, with highly pleomorphic or bizarre nuclei, and apoptotic bodies. About 35 mitotic events per one high-power field were counted. Necrotic areas represented 3–5% of the whole tumor volume. However, no sarcomatoid differentiation areas (characteristic of dedifferentiated chordoma) were observed.

Immunohistochemical stains (Figure2 C–F) showed a classic chordoma profile with cytoplasmic positivity for epithelial membrane antigen (EMA), S100 protein, Pan-Cytokeratin and strong nuclear Brachyury positivity. No GFAP or CD68 expression was observed. Ki67 proliferation index assessed manually and with the aid of AI algorithm resulted in around 15%.

3.2. HTS and therapeutic biomarkers assessment

The median read coverage was 870×, 619× and 2081× for the CCP, Oncomine TML and custom panel respectively. TMB was quiet, with 0.85 mutations/Mb. The CCP and Oncomine TML panels revealed only one pathogenic point mutation, stop-gain p.E564* in the *TSC1* gene. No pathogenic mutations were found in the custom panel with 25 epigenetic regulation genes. Regarding promoter mutations in the *TERT* gene and *MGMT* methylation status, no alterations were found.

3.3. Chromosomal microarray analysis (CMA)

In total, we discovered 180 regions with copy number variations (CNVs) in the chordoma tumor sample. The longest section was 58,014
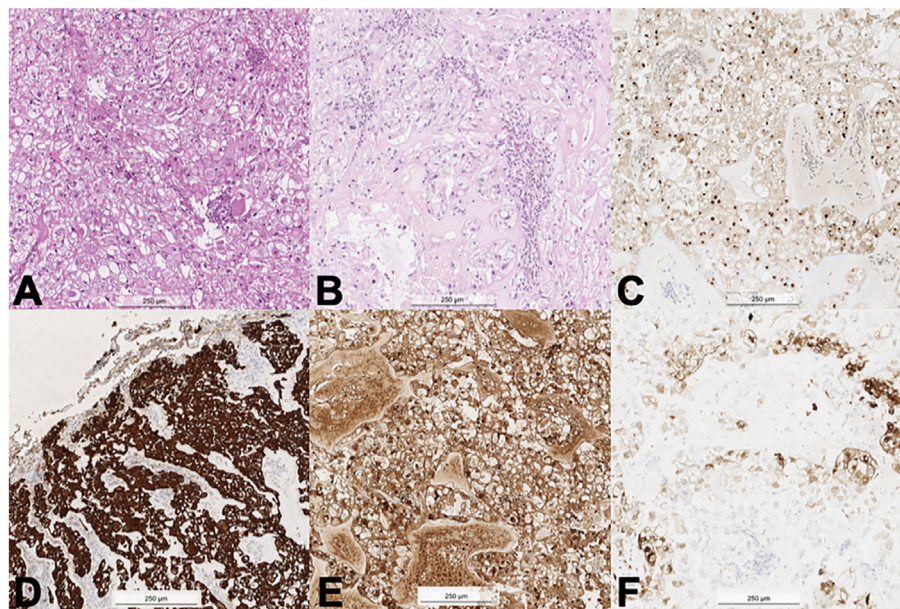
Figure 2. Clivus chordoma histopathology: H&E stain (A–B), tumor with characteristic physaliphorous cells, lobular architecture and abundant grayish-blue chondroid extracellular matrix; strong diffuse nuclear immunoreactivity for Brachyury (C); strong diffuse nuclear immunoreactivity for Pan-Cytokeratin (D), S100 (E), EMA (F). The scale bar is set to 200 μm.

kb long (arr[GRCh38] 9q21.31q34.3(79267492_137281464) × 1−2), harboring region 9q34 that includes *TSC1* gene, which, in combination with a point mutation p.E564* in *TSC1*, corresponds to a two-hit hypothesis of carcinogenesis in tuberous sclerosis. Further, 12 oncogenes [13] (Table 1) were located in amplified regions; 92 tumor suppressor genes [14] (Supplementary Material) were found in regions with loss status. According to dbEM database [15], we have registered copy number gains of four genes involved in epigenetic regulation – *ELP3*, *GTF3C4*, *MBD2* and *PHF2* (Table 1).

3.4. Pathway enrichment analysis

Gene set enrichment analysis revealed that the best enrichment score was obtained for the following biological processes: transposition regulation, deamination and nucleoside metabolism. The set of genes that causes these processes almost exclusively consists of the members of the APOBEC3 family (*APOBEC3A, APOBEC3B, APOBEC3C, APOBEC3D, APOBEC3F, APOBEC3G, APOBEC3H*). These genes are located closely within the chromosomal region 22q13.1, which is amplified in the studied sample in accordance with the CMA analysis (Figure 3).

4. Discussion

Herein we present uncommonly rare chordoma in the pediatric patient with TSC, an autosomal dominant disease characterized by multiple lesions and involvement of multiple organs of the body with birth

Table 1. Amplified oncogenes and genes that participate in epigenetic regulation found by CMA.

Amplified oncogenes found by CMA	
Genes	Microarray nomenclature of region
CBX7	arr[GRCh38] 22q13.1(38481456_39596655) × 2 − 3
DSG3	arr[GRCh38] 18q12.1(31429712_32174786) × 2 − 3
EMSY	arr[GRCh38] 11q13.4q13.5(75413088_76613978) × 2 − 3
FOXA1	arr[GRCh38] 14q13.3q21.1(36322204_38121000) × 2 − 3
KRAS	arr[GRCh38] 12p12.1(24902578_25984703) × 2 − 3
MIR633	arr[GRCh38] 17q23.2q23.3(62801615_63148876) × 2 − 3
NKX2-1	arr[GRCh38] 14q13.3q21.1(36322204_38121000) × 2 − 3
PDGFB	arr[GRCh38] 22q13.1(38481456_39596655) × 2 − 3
PRAME	arr[GRCh38] 22q11.21q11.22(21674445_23078872) × 2 − 3
ROCK1	arr[GRCh38] 18p11.21q11.1(14940734_21155391) × 2 − 3
SNAI1	arr[GRCh38] 20q13.13(49011068_50479891) × 2 − 3
ZFAS1	arr[GRCh38] 20q13.13(49011068_50479891) × 2 − 3
Altered genes that are involved in epigenetic regulation		

Genes	Microarray nomenclature	Description
ELP3	arr[GRCh38] 8p21.1p12(28068600_30351452) × 2 − 3	Histone Acetyl Transferases
GTF3C4	arr[GRCh38] 9q21.31q34.3(79267492_137281464) × 1 − 2	Histone Acetyl Transferases
MBD2	arr[GRCh38] 18q21.2(53697547_54220886) × 1 − 2	Chromatin Remodelers
PHF2	arr[GRCh38] 9q21.31q34.3(79267492_137281464) × 1 − 2	Histone Demethylases

Figure 3. GO biological process gene set enrichment analysis by using clusterProfiler R package [12].

prevalence between 1/6000 and 1/10,000 live births [16]. Since 1975, only 13 TSC-associated chordoma cases were described [3]. Chordomas are malignant slow-growing bone tumors thought to arise from vestigial or ectopic notochordal tissue [1]. The incidence of chordomas is currently estimated to be 0.8 cases per 1 million/year, which is lower than Ewing's sarcoma (1.7–4.4 cases per 1 million/year) [1, 2]. Most chordomas occur in people 40–60 years of age and have a slight predominance in men [1]. The majority of chordomas are intraosseous tumors involving the axial skeleton, affecting the base of skull/clivus, vertebral bodies, and sacrococcygeal bones in about equal proportions. On the other hand, pediatric chordomas, which occur before the age of 20 and take place in 5% of all cases, are usually developed within skull-based localization [2]. Chordoma associated with TSC differs from chordoma in the general pediatric population in the median age, where the diagnosis of TSC-associated chordomas is 6.2 months, whereas for chordoma in the general pediatric population it is set to 12 years [17]. The majority of TSC-associated chordomas are localized in the skull- and sacrum-based regions, and are uncommon in the spine, although this difference is most likely due to the small studied sample size [3, 17].

4.1. Histopathology

The current World Health Organization (WHO) "Classification of Soft Tissues and Bone" continues to classify chordoma into three types: conventional chordoma that includes a chondroid subtype, dedifferentiated chordoma, and a poorly differentiated chordoma [18]. The morphology varies between these subtypes, from the "physaliphorous cells" and myxoid matrix of the conventional type to the matrix that mimics hyaline cartilage in the chondroid subtype, to biphasic tumors with juxtaposed high-grade undifferentiated sarcomas in the dedifferentiated type [19, 20]. The poorly chordoma is characterized by highly undifferentiated morphology, prominent necrosis and the frequent absence of SMARCB1 (SNF5-homolog/SMARCB1, also known as INI1) expression [21, 22]. This type of tumor has been described in the pediatric population and is characterized by an aggressive clinical course [23, 24, 25]. All chordomas (except the dedifferentiated component in dedifferentiated and poorly differentiated chordoma) typically show positive immunohistochemical staining for keratins, Brachyury, S100, and EMA, whereas poorly differentiated chordoma is characterized by the absence of SMARCB1 expression [21, 22].

4.2. Recurrent alterations and involved pathways

Molecular genetics studies on chordomas have increased in recent years, but molecular genetic profiling using HTS and CMA of chordomas in patients with TSC has not yet been published. In contrast, much more data are available on sporadic chordomas, allowing for a more detailed analysis. It seems that point mutations are not frequent phenomena in chordomas. Studies show that chordoma tumor mutation burden (TMB) is mostly low, with a median of 0.53 mut/Mb and a range of 0.05–7.68 per tumor, however, tumors that harbor mutations in *PBRM1* have a higher overall burden of mutations and non-synonymous mutations [4]. On the other hand, chromosomal instability (CIN) is much more common, and recurrent CNVs are seen in chordomas [4, 26]. Recurrent losses are seen in 1p36 (*RUNX3*), 3p21 (*PBRM1, SETD2, BAP1*), 3q26 (*PIK3CA*), 6q25 (*ARID1B*), 9p21 (*CDKN2A, CDKN2B, MTAP*), 10q23 (*PTEN*), 11q22 (*ATM*), 22q12 (*CHEK2*), 22q11 (*SMARCB1*), but also gains in 6q27 (*Brachyury*), 7q31 (*MET*), chromosomes 7 and 19 [27,28]. CNVs can also be clustered by different profiles of CNVs, from a group with an almost completely altered genome, to a group where there are almost no alterations [4]. Currently, studies show that altered *PBRM1, SETD2, CDKN2A/B*, and *LYST* genes account for about 34% of the analyzed cohort of chordomas [4, 26, 29]. These findings suggest that epigenetic dysregulation, via chromatin remodeling (*PBRM1, SETD2*), may play an important role in chordoma pathogenesis [4]. Overall, studies show that chordomas are characterized by CIN and/or alterations involving genes

of the PI3K-AKT signaling pathway and chromatin remodeling genes [4, 26, 29].

Our sample, apart from a small number of point mutations, has chromosomal instability, in which we found one recurrent CNV carrying the *ATM* gene (Supplementary Material). We found that 9q region, where *TSC1* gene is located (9q34), has loss status, leading to biallelic inactivation of *TSC1* (due to the p.E564*point mutation), which in turn involves the mTOR signaling pathway; all of which makes sense for patients with TSC. Involvement of *PBRM1, SETD2, CDKN2A/B, LYST* or *TBXT* has not been found, however, we detected a loss in 18q21.2 region, where the *MBD2* gene involved in chromatin remodeling is located [30] and gains that involve several oncogenes – *CBX7, FOXA1, EMSY* - that also indirectly affect chromatin (Table 1). Notably, CBX7, one component of the Polycomb group (PcG) multiprotein PRC1-like complex, through recruitment and/or activation of the HMTase SUV39H2, initiates trimethylation of H3K9 (H3K9me3) at the p16-Arf locus leading to epigenetic inactivation of *p16* (*CDKN2A*) [31], which might lead to inactivation of *CDKN2A* in our case. In addition, PcGs proteins are epigenetic modifiers and are essential for the correct development and differentiation of the nervous system [32].

APOBEC signatures have been shown to be detected in distant metastatic chordoma specimens and absent in recurrent tumors [4]. Higher fractions of APOBEC mutational signatures were observed in tumors with PBRM1+ in comparison with PBRM1-tumors [4]. APOBEC3 proteins are cytidine deaminases that govern a wide spectrum of genomic and epigenomic modifications [33]. APOBEC3 enzymes are well-known players in the innate immune response to viral infections and are acting as restriction factors for diverse viruses, including hepatitis B virus, human T-cell leukemia virus, parvoviruses and human papillomavirus [33]. It is also known that APOBEC family proteins are able to restrict exogenous retroviruses as well [34]. Along with ADAR enzymes, members of the AID/APOBEC protein family play a crucial role in cell defense against L1 retrotransposons activity [35]. However, APOBEC3 proteins contribute to human cancer by eliciting cellular DNA damage responses. Evidence of APOBEC3-mediated mutagenesis and its contribution to DNA replication stress and chromosomal instability has been demonstrated in recent studies [36, 37]. The C→T transitions in the TC context are thought to be a mutational signature of *APOBEC3* in cancer genomes caused by endogenous APOBEC3A and APOBEC3B activity [38]. The results of the gene set enrichment analysis showed that the highest enrichment score in the case described here was for biological processes involving APOBEC3. Amplification of the 22q13.1 region (arr[GRCh38] 22q13.1(38481456_39596655) × 2 − 3) with *APOBEC3* could explain CIN in our case, but we could not detect the *APOBEC* mutational signature due to the low number of point mutations, which is also reflected in the TMB, set at 0.85 mut/Mb.

4.3. Survival and therapy

4.3.1. Survival

According to the Surveillance, Epidemiology, and End Results (SEER) program, the median survival time of chordomas is 6.3 years. Survival at 5, 10 and 20 years was 98%, 40% and 13% respectively. For pediatric chordomas, overall 5-year and 10-year survival rates were 66.6% and 58.6%, and progression-free survival rates were 55.7% and 52 %, respectively [1]. Survival curve analysis (chordoma-specific survival) in relation to some regions with alterations (CNVs that affect *SWI/SNF* genes and deletion in 22q) were associated with positive outcomes [4]. With regard to recurrence-free survival, positive outcomes were observed in the absence of such alterations affecting the *SWI/SNF* genes, p21.3 deletion, 9q21.11 deletion, and 22q deletion [4]. It has also been shown that mutations in the *TERT* promoter region are present in 8.7 % of chordomas and correlate with better survival [39]. We analyzed the *TERT* promoter region in our sample and found no mutations that are associated with better survival (Supplementary Material). To date, 14 cases of chordomas have been described, including this case, of which only one patient died at the age of 6 years, and no correlation with mutations has been reported [17, 40].

4.3.2. Therapy

Chordomas are now known to be genetically heterogeneous tumors. According to the National Comprehensive Cancer Network (NCCN) guidelines, the primary treatment of chordomas is wide excision with adequate margins. If chordoma is unresectable, radiotherapy is considered. Chordomas are not amenable to chemotherapy, but the involvement of PDGFR, EGFR and mTOR in the pathological processes has led to the development of targeted treatments for chordomas. Monotherapy with tyrosine kinase inhibitors (TKIs), such as imatinib, erlotinib or sorafenib, is recommended as the first-line treatment [5]. Combination therapy (two TKIs or TKIs plus an mTOR inhibitor) has proven effective in patients with advanced chordoma resistant to monotherapy [5]. Current preclinical results of a recombinant *Saccharomyces cerevisiae* (yeast) vaccine encoding brachyury (GI-6301) demonstrated that 7/11 patients showed no evidence of disease progression at five months [5]. Yang et al. also showed that vismodegib, an antagonist of the Shh-Gli1 signaling pathway, induces apoptosis and G1/S cell cycle arrest in chordoma cells and effectively suppresses chordoma xenograft growth [41].

In our sample, EGFR-activating mutations were not detected by HTS or RT-PCR. However, we found an amplified *KRAS* gene that may confer resistance to anti-EGFR therapy [42] in relation to the efficacy of TKI monotherapy in chordomas. Methylation of the *MGMT* promoter, which is known to be a prognostic and predictive marker for patients with glioblastoma and tumor response to temozolomide (TMZ) chemotherapy [43], has been observed in 26.6% of recurrent clival chordomas, suggesting the potential use of TMZ chemotherapy [44, 45]. No methylation of *MGMT* promoter region was identified in our sample. Regarding immunotherapy, most chordomas have a low TMB (~0.53 mut/Mb), corresponding to "cold tumors" and suggesting the ineffectiveness of immunotherapy [4, 46]. However, in another case report study of spinal chordoma with low TMB (6.9 mut/Mb), negative for PD-L1 expression and with a frameshift mutation in *PBRM1*, the use of pembrolizumab, an immune checkpoint inhibitor targeting the PD-1 receptor on lymphocytes, showed a 9.3-month increase in progression-free survival compared to imatinib (9 months) and nitro-camptothecin (3 months) [47]. In our clivus chordoma sample, TMB was also low, with 0.85 mut/Mb, and there were no point mutations or indels in the *PBRM1* gene.

To our knowledge, possible epigenetic inactivation of *CDKN2A* due to amplification of *CBX7* has not previously been observed in chordomas. CDKN2A activates the Rb and CDK4/6 pathways, which in turn are highly expressed in the chordoma tissue cell line [5, 48]. Palbociclib, which is a CDK4/6 inhibitor, is currently in phase II clinical trial for patients with chordoma (NCT03110744). In relation to APOBEC, as for tumor therapy, attempts have been made regarding A3B inhibition as therapy by hypomutation, or therapy by hypermutation where in the latter case, boosting mutational burden in the cells to toxic levels, through small molecule agonism of A3-catalyzed mutation, might accelerate cancer cell death [6]. These and other molecular genetic clues may shed light on the shortcomings of current clinical approaches to the treatment of chordomas and potentially improve therapy on a case-by-case basis, i.e. precision medicine.

5. Conclusion

Here we described the 14th case of a patient with tuberous sclerosis complex who has a clivus chordoma. In this tumor, in addition to biallelic inactivation of the *TSC1* gene, we found chromosomal instability, amplification of several oncogenes, including *KRAS* and *CBX7* genes, and alterations of epigenetic regulation genes. Chromosomal instability and involvement of epigenetic regulation genes are common in chordomas. Inactivation of *CDKN2A* is also common, however, its epigenetic inactivation due to amplification of *CBX7* has not yet been described in chordomas. Through enrichment analysis, we showed the involvement of *APOBEC3*, which has also not been previously described in chordomas. APOBEC3s are involved in chromosomal instability, which may explain its frequent occurrence among chordomas and can be considered as a target in hypo- or hypermutation for cancer therapies in the future. Regarding targeted therapy, we did not identify mutations in *EGFR*, however, the gain status of *KRAS* may indicate the ineffectiveness of EGFR monotherapy, which has been shown to be effective in the treatment of chordomas. We believe that a detailed molecular genetic analysis, even in a single case, may help to understand the genetic and molecular features of childhood chordomas associated with TSC and assist in the search for targeted treatment options.

Declarations

Author contribution statement

All authors listed have significantly contributed to the investigation, development and writing of this article.

Data availability statement

Data associated with this study has been deposited at https://www.ncbi.nlm.nih.gov/geo/, GSE196823; https://www.ncbi.nlm.nih.gov/, PRJNA799928.

Declaration of interest's statement

The authors declare the following conflict of interests: Maxim Untesco was employed by the company UNIM Ltd. The remaining authors declare that the research was conducted in the absence of any commercial or financial relationships that could be construed as a potential conflict of interest.

Additional information

Supplementary content related to this article has been published online at https://doi.org/10.1016/j.heliyon.2022.e10291.

References

[1] Karpathiou, G., Dumollard, J.M., Dridi, M., Dal Col, P., Barral, F.-G., Boutonnat, J., Peoc'h, M. Chordomas, 2020. A review with emphasis on their pathophysiology, pathology, molecular biology, and genetics. Pathol. Res. Pract. 216, 153089.

[2] Ulici, V., Hart, J., 2022 Mar 1. Chordoma. Arch. Pathol. Lab. Med. 146 (3), 386–395.

[3] Dahl, N.A., Luebbert, T., Loi, M., Neuberger, I., Handler, M.H., Kleinschmidt-DeMasters, B.K., Mulcahy Levy, J.M., 2017. Chordoma occurs in young children with tuberous sclerosis. J. Neuropathol. Exp. Neurol. 76, 418–423.

[4] Bai, J., Shi, J., Li, C., Wang, S., Zhang, T., Hua, X., Zhu, B., Koka, H., Wu, H.-H., Song, L., Wang, D., Wang, M., Zhou, W., Ballew, B.J., Zhu, B., Hicks, B., Mirabello, L., Parry, D.M., Zhai, Y., Li, M., Yang, X.R., 2021. Whole genome sequencing of skull-base chordoma reveals genomic alterations associated with recurrence and chordoma-specific survival. Nat. Commun. 12, 757.

[5] Meng, T., Jin, J., Jiang, C., Huang, R., Yin, H., Song, D., Cheng, L., 2019. Molecular targeted therapy in the treatment of chordoma: A systematic review. Front. Oncol. 9, 30.

[6] Olson, M.E., Harris, R.S., Harki, D.A., 2018. APOBEC enzymes as targets for virus and cancer therapy. Cell Chem. Biol. 25, 36–49.

[7] Harris, R.S., 2008. Enhancing immunity to HIV through APOBEC. Nat. Biotechnol. 26, 1089–1090.

[8] Ferraresi, V., Nuzzo, C., Zoccali, C., Marandino, F., Vidiri, A., Salducca, N., Zeuli, M., Giannarelli, D., Cognetti, F., Biagini, R., 2010. Chordoma: clinical characteristics, management and prognosis of a case series of 25 patients. BMC Cancer 10, 22.

[9] Radaelli, S., Fossati, P., Stacchiotti, S., Akiyama, T., Asencio, J.M., Bandiera, S., Boglione, A., Boland, P., Bolle, S., Bruland, Ø., Brunello, A., Bruzzi, P., Campanacci, D., Cananzi, F., Capanna, R., Casadei, R., Cordoba, A., Court, C., Dei Tos, A.P., DeLaney, T.F., Gronchi, A., 2020. The sacral chordoma margin. Eur. J. Surg. Oncol. 46, 1415–1422.

[10] Wang, K., Li, M., Hakonarson, H., 2010. Annovar: functional annotation of genetic variants from high-throughput sequencing data. Nucleic Acids Res 38, e164.

[11] Robinson, J.T., Thorvaldsdóttir, H., Wenger, A.M., Zehir, A., Mesirov, J.P., 2017. Variant Review with the Integrative Genomics Viewer. Cancer Res 77, e31–e34.

[12] Yu, G., Wang, L.-G., Han, Y., He, Q.-Y., 2012. clusterProfiler: an R package for comparing biological themes among gene clusters. OMICS 16, 284–287.

[13] Liu, Y., Sun, J., Zhao, M. Ongene, 2017. A literature-based database for human oncogenes. J. Genet. Genomics 44, 119–121.

[14] Zhao, M., Kim, P., Mitra, R., Zhao, J., Zhao, Z., 2016. TSGene 2.0: an updated literature-based knowledgebase for tumor suppressor genes. Nucleic Acids Res 44, D1023–D1031.

[15] Singh Nanda, J., Kumar, R., Raghava, G.P.S. dbem, 2016. A database of epigenetic modifiers curated from cancerous and normal genomes. Sci. Rep. 6, 19340.

[16] Fujimoto, A., Okanishi, T., Imai, S., Ogai, M., Fukunaga, A., Nakamura, H., Sato, K., Obana, A., Masui, T., Arai, Y., Enoki, H., 2018. Establishment of a Regional Interdisciplinary Medical System for Managing Patients with Tuberous Sclerosis Complex (TSC). Sci. Rep. 8, 16747.

[17] McMaster, M.L., Goldstein, A.M., Parry, D.M., 2011. Clinical features distinguish childhood chordoma associated with tuberous sclerosis complex (TSC) from chordoma in the general paediatric population. J. Med. Genet. 48, 444–449.

[18] Franceschi, E., Frappaz, D., Rudà, R., Hau, P., Preusser, M., Houillier, C., Lombardi, G., Asioli, S., Dehais, C., Bielle, F., Di Nunno, V., van den Bent, M., Brandes, A.A., Idbaih, A., 2020. EURACAN Domain 10 Rare primary central nervous system tumors in adults: an overview. Front. Oncol. 10, 996.

[19] Hung, Y.P., Diaz-Perez, J.A., Cote, G.M., Wejde, J., Schwab, J.H., Nardi, V., Chebib, I.A., Deshpande, V., Selig, M.K., Bredella, M.A., Rosenberg, A.E., Nielsen, G.P., 2020. Dedifferentiated chordoma: clinicopathologic and molecular characteristics with integrative analysis. Am. J. Surg. Pathol. 44, 1213–1223.

[20] Asioli, S., Zoli, M., Guaraldi, F., Sollini, G., Bacci, A., Gibertoni, D., Ricci, C., Morandi, L., Pasquini, E., Righi, A., Mazzatenta, D., 2020. Peculiar pathological, radiological and clinical features of skull-base de-differentiated chordomas. Results from a referral centre case-series and literature review. Histopathology 76, 731–739.

[21] Shih, A.R., Cote, G.M., Chebib, I., Choy, E., DeLaney, T., Deshpande, V., Hornicek, F.J., Miao, R., Schwab, J.H., Nielsen, G.P., Chen, Y.-L., 2018. Clinicopathologic characteristics of poorly differentiated chordoma. Mod. Pathol. 31, 1237–1245.

[22] Hasselblatt, M., Thomas, C., Hovestadt, V., Schrimpf, D., Johann, P., Bens, S., Oyen, F., Peetz-Dienhart, S., Crede, Y., Wefers, A., Vogel, H., Riemenschneider, M.J., Antonelli, M., Giangaspero, F., Bernardo, M.C., Giannini, C., Ud Din, N., Perry, A., Keyvani, K., van Landeghem, F., Kool, M., 2016. Poorly differentiated chordoma with SMARCB1/INI1 loss: a distinct molecular entity with dismal prognosis. Acta Neuropathol 132, 149–151.

[23] Tauziéde-Espariat, A., Bresson, D., Polivka, M., Bouazza, S., Labrousse, F., Aronica, E., Pretet, J.-L., Projetti, F., Herman, P., Salle, H., Monnien, F., Valmary-Degano, S., Laquerrière, A., Pocard, M., Chaigneau, L., Isambert, N., Aubriot-Lorton, M.-H., Feuvret, L., George, B., Froelich, S., Adle-Biassette, H., 2016. Prognostic and therapeutic markers in chordomas: A study of 287 tumors. J. Neuropathol. Exp. Neurol. 75, 111–120.

[24] Zheng, W., Huang, Y., Guan, T., Lu, S., Yao, L., Wu, S., Chen, H., Wang, N., Liang, Y., Xiao, W., Jiang, X., Wen, S., 2019. Application of nomograms to predict overall and cancer-specific survival in patients with chordoma. J. Bone Oncol. 18, 100247.

[25] Beccaria, K., Tauziède-Espariat, A., Monnien, F., Adle-Biassette, H., Masliah-Planchon, J., Pierron, G., Maillot, L., Polivka, M., Laquerrière, A., Bouillot-Eimer, S., Gimbert, E., Gauchotte, G., Coffinet, L., Sevestre, H., Alapetite, C., Bolle, S., Thompson, D., Bouazza, S., George, B., Zérah, M., Varlet, P., 2018. Pediatric chordomas: results of a multicentric study of 40 children and proposal for a histopathological prognostic grading system and new therapeutic strategies. J. Neuropathol. Exp. Neurol. 77, 207–215.

[26] Tarpey, P.S., Behjati, S., Young, M.D., Martincorena, I., Alexandrov, L.B., Farndon, S.J., Guzzo, C., Hardy, C., Latimer, C., Butler, A.P., Teague, J.W., Shlien, A., Futreal, P.A., Shah, S., Bashashati, A., Jamshidi, F., Nielsen, T.O., Huntsman, D., Baumhoer, D., Brandner, S., Campbell, P.J., 2017. The driver landscape of sporadic chordoma. Nat. Commun. 8, 890.

[27] Liu, C., Liu, A., Bettegowda, C., 2021. Molecular morphogenesis and genetic mechanisms of spinal chordoma. In: Sciubba, D.M., Schwab, J.H. (Eds.), Chordoma of the spine: A comprehensive review. Springer International Publishing, Cham, pp. 13–29.

[28] Le, L.P., Nielsen, G.P., Rosenberg, A.E., Thomas, D., Batten, J.M., Deshpande, V., Schwab, J., Duan, Z., Xavier, R.J., Hornicek, F.J., Iafrate, A.J., 2011. Recurrent chromosomal copy number alterations in sporadic chordomas. PLoS ONE 6, e18846.

[29] Noor, A., Bindal, P., Ramirez, M., Vredenburgh, J. Chordoma, 2020. A case report and review of literature. Am. J. Case Rep. 21, e918927.

[30] Menafra, R., Stunnenberg, H.G., 2014. MBD2 and MBD3: elusive functions and mechanisms. Front. Genet. 5, 428.

[31] Li, Q., Wang, X., Lu, Z., Zhang, B., Guan, Z., Liu, Z., Zhong, Q., Gu, L., Zhou, J., Zhu, B., Ji, J., Deng, D., 2010. Polycomb CBX7 directly controls trimethylation of histone H3 at lysine 9 at the p16 locus. PLoS ONE 5, e13732.

[32] Desai, D., Pethe, P., 2020. Polycomb repressive complex 1: Regulators of neurogenesis from embryonic to adult stage. J. Cell. Physiol. 235, 4031–4045.

[33] Harris, R.S., Dudley, J.P., 2015. APOBECs and virus restriction. Virology 479–480, 131–145.

[34] Mavragani, C.P., Kirou, K.A., Nezos, A., Seshan, S., Wild, T., Wahl, S.M., Moutsopoulos, H.M., Crow, M.K., 2021. Expression of APOBEC family members as regulators of endogenous retroelements and malignant transformation in systemic autoimmunity. Clin. Immunol. 223, 108649.

[35] Orecchini, E., Frassinelli, L., Galardi, S., Ciafrè, S.A., Michienzi, A., 2018. Post-transcriptional regulation of LINE-1 retrotransposition by AID/APOBEC and ADAR deaminases. Chromosome Res 26, 45–59.

[36] Yamazaki, H., Shirakawa, K., Matsumoto, T., Hirabayashi, S., Murakawa, Y., Kobayashi, M., Sarca, A.D., Kazuma, Y., Matsui, H., Maruyama, W., Fukuda, H., Shirakawa, R., Shindo, K., Ri, M., Iida, S., Takaori-Kondo, A., 2019. Endogenous APOBEC3B overexpression constitutively generates DNA substitutions and deletions in myeloma cells. Sci. Rep. 9, 7122.

[37] Venkatesan, S., Angelova, M., Puttick, C., Zhai, H., Caswell, D.R., Lu, W.-T., Dietzen, M., Galanos, P., Evangelou, K., Bellelli, R., Lim, E.L., Watkins, T.B.K., Rowan, A., Teixeira, V.H., Zhao, Y., Chen, H., Ngo, B., Zalmas, L.-P., Al Bakir, M., Hober, S., 2021. TRACERx Consortium Induction of APOBEC3 exacerbates DNA replication stress and chromosomal instability in early breast and lung cancer evolution. Cancer Discov. 11, 2456–2473.

[38] Chan, K., Roberts, S.A., Klimczak, L.J., Sterling, J.F., Saini, N., Malc, E.P., Kim, J., Kwiatkowski, D.J., Fargo, D.C., Mieczkowski, P.A., Getz, G., Gordenin, D.A., 2015. An APOBEC3A hypermutation signature is distinguishable from the signature of background mutagenesis by APOBEC3B in human cancers. Nat. Genet. 47, 1067–1072.

[39] Bettegowda, C., Yip, S., Jiang, B., Wang, W.-L., Clarke, M.J., Lazary, A., Gambarotti, M., Zhang, M., Sciubba, D.M., Wolinsky, J.-P., Goodwin, C.R., McCarthy, E., Germscheid, N.M., Sahgal, A., Gokaslan, Z.L., Boriani, S., Varga, P.P., Fisher, C.G., Rhines, L.D., 2019. Prognostic significance of human telomerase reverse transcriptase promoter region mutations C228T and C250T for overall survival in spinal chordomas. Neuro Oncol 21, 1005–1015.

[40] Börgel, J., Olschewski, H., Reuter, T., Miterski, B., Epplen, J.T., 2001. Does the tuberous sclerosis complex include clivus chordoma? A case report. Eur. J. Pediatr. 160, 138.

[41] Yang, C., Yong, L., Liang, C., Li, Y., Ma, Y., Wei, F., Jiang, L., Zhou, H., He, G., Pan, X., Hai, B., Wu, J., Xu, Y., Liu, Z., Liu, X., 2020. Genetic landscape and ligand-dependent activation of sonic hedgehog-Gli1 signaling in chordomas: a novel therapeutic target. Oncogene 39, 4711–4727.

[42] Favazza, L.A., Parseghian, C.M., Kaya, C., Nikiforova, M.N., Roy, S., Wald, A.I., Landau, M.S., Proksell, S.S., Dueker, J.M., Johnston, E.R., Brand, R.E., Bahary, N., Gorantla, V.C., Rhee, J.C., Pingpank, J.F., Choudry, H.A., Lee, K., Paniccia, A., Ongchin, M.C., Zureikat, A.H., Singhi, A.D., 2020. KRAS amplification in metastatic colon cancer is associated with a history of inflammatory bowel disease and may confer resistance to anti-EGFR therapy. Mod. Pathol. 33, 1832–1843.

[43] Katsigiannis, S., Grau, S., Krischek, B., Er, K., Pintea, B., Goldbrunner, R., Stavrinou, P., 2021. MGMT-Positive vs MGMT-Negative Patients With Glioblastoma: Identification of Prognostic Factors and Resection Threshold. Neurosurgery 88, E323–E329.

[44] Mansouri, A., Hachem, L.D., Mansouri, S., Nassiri, F., Laperriere, N.J., Xia, D., Lindeman, N.I., Wen, P.Y., Chakravarti, A., Mehta, M.P., Hegi, M.E., Stupp, R., Aldape, K.D., Zadeh, G., 2019. MGMT promoter methylation status testing to guide therapy for glioblastoma: refining the approach based on emerging evidence and current challenges. Neuro Oncol 21, 167–178.

[45] Marucci, G., Morandi, L., Mazzatenta, D., Frank, G., Pasquini, E., Foschini, M.P., 2014. MGMT promoter methylation status in clival chordoma. J Neurooncol 118, 271–276.

[46] Maleki Vareki, S., 2018. High and low mutational burden tumors versus immunologically hot and cold tumors and response to immune checkpoint inhibitors. J. Immunother. Cancer 6, 157.

[47] Wu, X., Lin, X., Chen, Y., Kong, W., Xu, J., Yu, Z., 2020. Response of metastatic chordoma to the immune checkpoint inhibitor pembrolizumab: A case report. Front. Oncol. 10, 565945.

[48] Bosotti, R., Magnaghi, P., Di Bella, S., Cozzi, L., Cusi, C., Bozzi, F., Beltrami, N., Carapezza, G., Ballinari, D., Amboldi, N., Lupi, R., Somaschini, A., Raddrizzani, L., Salom, B., Galvani, A., Stacchiotti, S., Tamborini, E., Isacchi, A., 2017. Establishment and genomic characterization of the new chordoma cell line Chor-IN-1. Sci. Rep. 7, 9226.